CHAPTER SEVEN

DISCUSSION

7.1 INTRODUCTION

In this chapter, the results of the characterisation of Smorgon Steel Works dust and of the reduction treatment by the iron-reduction distillation process from Chapter Six are discussed. Section 7.2 discusses the formation and characterisation of the EAF dust. The results from laboratory experiments are discussed as a function of the operating parameters and compared with previous work. The discussions of the results obtained from the first reduction stage are given in Section 7.3 . The second reduction stage results and possible kinetic models for reduction of zinc oxide by metallic iron in both nitrogen atmosphere and under vacuum are discussed in Section 7.4.

7.2 FORMATION AND CHARACTERISATION OF SMORGON STEEL WORKS DUST

Smorgon Steel Works EAF dust is very fine-grained and required high magnifications (500-5000X) of the SEM for mineral identification, textural analysis and microscopic study. EAF dust is formed by vaporisation, melt explosion atomisation and by carry-over from charge materials. Volatile metals such as lead, cadmium and zinc are easily vaporised at the temperatures of the EAF furnace. Therefore, the oxidation of these vaporised metals form the extremely small dust fractions. Lime, calcite and coke/graphite are from the direct carry-over of the initial charge materials.

The chemical composition of Smorgon Steel Works EAF dust is extremely site-specific, due to differences in scrap feed composition. Smorgon Steel Works dust composition

varies from time to time. Zinc and iron are the main elements present. The compounds formed from the zinc and iron account for approximately 70 percent by weight of the dust. Of the hazardous elements, lead is usually about 1-4 percent and cadmium 0.02-0.15 percent. Chlorine is present in the form of soluble salts of sodium and potassium chloride that are leachable from EAF by hot water leaching or volatilised at the reduction temperature.

Figure 6.3 shows the magnetite and zinc oxide particles which are not in contact with each other. XRD analysis of Smorgon Steel Works dust showed that the dominant phases are a spinel group presented as zinc ferrite and magnetite. Another form of zinc is present as zinc oxide. From these results, magnetite and zinc oxide are present as particles, the phases between two of these particles would be agglomerated zinc ferrite and minor elements which cannot be distinguished from these phases.

Figure D4 (see page 112) of Appendix D shows the XRDPs of EAF dust after dilute sulphuric acid leaching. The zinc oxide peaks have decreased. The results show that not all of the zinc oxide was leached from the EAF dust. The zinc oxide percentage should be more than that indicated in Table 6.3 (see page 62) and may be as high as 10.0 percent.

According to Table 6.3 (see page 62), about 40 percent of the compounds present as zinc ferrite which is different from the compounds present in the steelmaking dust used in the work of Itoh and Azakami (1994). No information was provided on the concentration of the different phases present in their work. However, their work was based on the reduction of reagent grade zinc oxide by hematite and they assumed that the zinc in their steelmaking dust was in the form of zinc oxide.

7.3 FIRST REDUCTION STAGE ANALYSIS

7.3.1 Effect of Temperature and Time

The results in Figure 6.4 (see page 63) represented the fractional reduction of iron oxide to metallic iron obtained by dissolving the residues in bromine-methanol solution and the XRDPs in Figure D4 (see page 112) show that iron oxide in the form of magnetite and spinel zinc ferrite was reduced to metallic iron. According to the results in Figure 6.4 (see page 63), when the temperature increased the fractional reduction of iron also increased. The results show that at 700 and 800 °C the fractional reduction of iron seems to be identical but was retarded at 94-97 percent reduction, which was considered to be due to the formation of cementite (Fe_3C). Cementite can be formed by the reduction of wustite and magnetite at temperature about 700 °C according to the following reactions as stated before on page 39 :

$$3FeO_{(s)} + 5CO_{(g)} = Fe_3C_{(s)} + 4CO_{2(g)} \quad (4.8)$$

$$Fe_3O_{4(s)} + 6CO_{(g)} = Fe_3C_{(s)} + 5CO_{2(g)} \quad (4.9)$$

Figure 7.1 compares the fractional reduction of iron of Itoh and Azakami with the present work. The Itoh and Azakami results were obtained from steelmaking dust reduced at 700 and 800 °C using CO/CO_2 gas ratio of 10 . Although there seems to be some difference between Itoh and Azakami and the present results, a similar trend was observed at both operating temperatures. In the present work, the iron in the unreacted EAF dust was 37.20 percent but was 20.10 percent in the Itoh and Azakami dust sample. As stated before, no information was given on the concentration of the different phases present in their work. The Itoh and Azakami results in Figure 2.9 (see page 29) showed that in the reagent grade sample, the reduction rate was slower than with calcine and steelmaking dust. However, hematite was the only iron source and no zinc ferrite was present in the reagent grade sample. Therefore, the reduction rates of the present work were faster than those of Itoh and Azakami work possibly because the zinc ferrite/magnetite ratio in the EAF dust used in the present work was larger than the ratio in the Itoh and Azakami steelmaking dust sample.

Rosenqvist (1983) states that in roasted zinc ores contained various impurities and other zinc compounds such as ferrite, since iron is more noble than zinc, zinc ferrite will react below 900 °C according to the reaction :

$$ZnO.Fe_2O_{3\,(s)} + 3CO_{(g)} = ZnO_{(s)} + 2Fe_{(s)} + 3CO_{2\,(g)} \quad (7.1)$$

Latkowska and Ptak (1987) found that in the reduction of synthetic zinc ferrite using CO/CO_2 gas ratios of 0.33, 1.0 and 3.0 and temperatures between 950 and 1200 °C, the hematite in the spinel zinc ferrite was reduced to wustite, which was the stable reaction product under every conditions. The appearance of zinc oxide in the products depended on the temperature and the reduction time.

For the two studies of Rosenqvist (1983) and Latkowska and Ptak (1987), it can be said that at 700 - 800 °C and $CO/CO_2 = 9$, spinel zinc ferrite is reduced by carbon monoxide to zinc oxide and wustite. Under these conditions, zinc oxide cannot be reduced to metallic zinc, but wustite is not stable. Then wustite is reduced by carbon monoxide to metallic iron according to the reactions as stated before in Chapter 4 (see page 42) :

$$ZnO.Fe_2O_{3\,(s)} + CO_{(g)} = ZnO_{(s)} + 2FeO_{(s)} + CO_{2\,(g)} \quad (4.14)$$

$$FeO_{(s)} + CO_{(g)} = Fe_{(s)} + CO_{2\,(g)} \quad (4.16)$$

Reaction 7.1 is the same as the reaction obtained from the combination of Reactions 4.14 and 4.16 .

In this reduction stage, the cadmium percentage decreased after reduction while the other minor elements were unchanged. The reduced briquette was examined by the ICP-AES method and the result (Table 6.4) confirms that cadmium percentage decreased from 0.021 percent by weight to <18 ppm. The zinc percentage decreased about 0.65 percent. Therefore, the first reduction stage conditions are suitable for obtaining metallic iron.

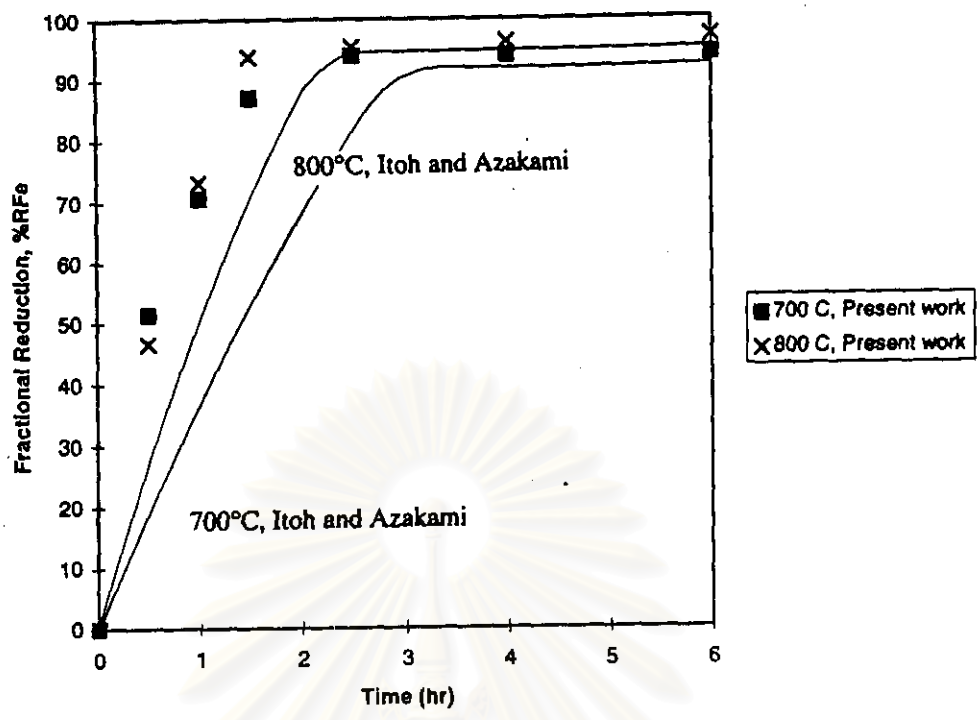

Figure 7.1: Comparison of the first reduction stage results.

7.3.2 Effect of Gas Composition

In this first reduction stage, the gas composition was made up of a mixture of carbon monoxide and carbon dioxide. The strength of the carbon monoxide reducing gas was decreased by the presence of the carbon dioxide gas. Therefore the reactant gas composition is expected to have an effect on the reduction kinetics.

The effect of the ratio of carbon monoxide/carbon dioxide gas composition on the reduction of iron oxide obtained from Figure 6.5 (see page 65) shows that the larger CO/CO_2 gas ratio gave a faster reduction rate of magnetite and hematite in zinc ferrite. Because the driving force for reduction is the difference between the partial pressure of the reducing gas and its partial pressure at equilibrium, these results are to be expected in as much as the presence of carbon monoxide decreases the concentration of carbon dioxide. That means, the reactant gas mixture should have the maximum concentration possible in carbon monoxide.

On the other hand, the presence of carbon dioxide may produce more carbon. Carbon can react with metallic iron to form cementite which may retard the reduction rate above about 70 percent for the CO/CO_2 gas ratio of 3 .

7.3.3 Effect of Sintering Process

The briquette obtained from sintering process produced zinc ferrite and magnetite as the major phases. The results in Figure 6.6 (see page 66) shows that the reduction rate of the sintered briquette was lower than the non-sintered briquette in the first two and a half hours of reduction time but after that the reduction rate was quite similar. The zinc oxide phase which originally was 7.80 percent by weight reacted with hematite during the sintering process at 1100 °C. This confirms that the zinc ferrite is reduced by carbon monoxide during the first reduction stage because zinc oxide in the non-sintered briquette is not reduced under the first stage conditions.

The sintered briquette is more dense and has a stronger structure than the non-sintered briquette. Therefore at the beginning of reduction, the reactant gas diffuses through the briquette and reacts with iron oxide at a slower rate than the non-sintered briquette which has more porosity. However, the sintering process is also recommended to give a stronger structure of the briquette or pellet when the process is carried out at the commercial scale.

7.4 SECOND REDUCTION STAGE ANALYSIS

7.4.1 Effect of Temperature and Time

According to the results in Figure 6.7 and 6.8 (see page 68-69), zinc oxide was preferentially reduced by metallic iron obtained from the first reduction stage to zinc vapour. When the temperature increased the fractional reduction of zinc also increased in both the nitrogen atmosphere and under vacuum.

Figure 6.9 shows that at the same temperature, in a nitrogen atmosphere the reduction rate was very slow. Most of the zinc oxide was reduced within 82 and 40 minutes under vacuum but required 7 and 4 hours in a nitrogen atmosphere at 900 and 1000 °C, respectively. These results indicate that the transfer of zinc vapour from the briquette surface to a nitrogen atmosphere or vacuum has a major effect on the kinetics of the reduction of the zinc oxide with metallic iron.

Figure 7.2 compares the present work with the fractional reduction of zinc from Itoh and Azakami. The results of Itoh and Azakami were obtained from steelmaking dust reduction at 900 and 1000 °C under a vacuum of 10^{-5} atm. A lower vacuum gives faster reduction rates.

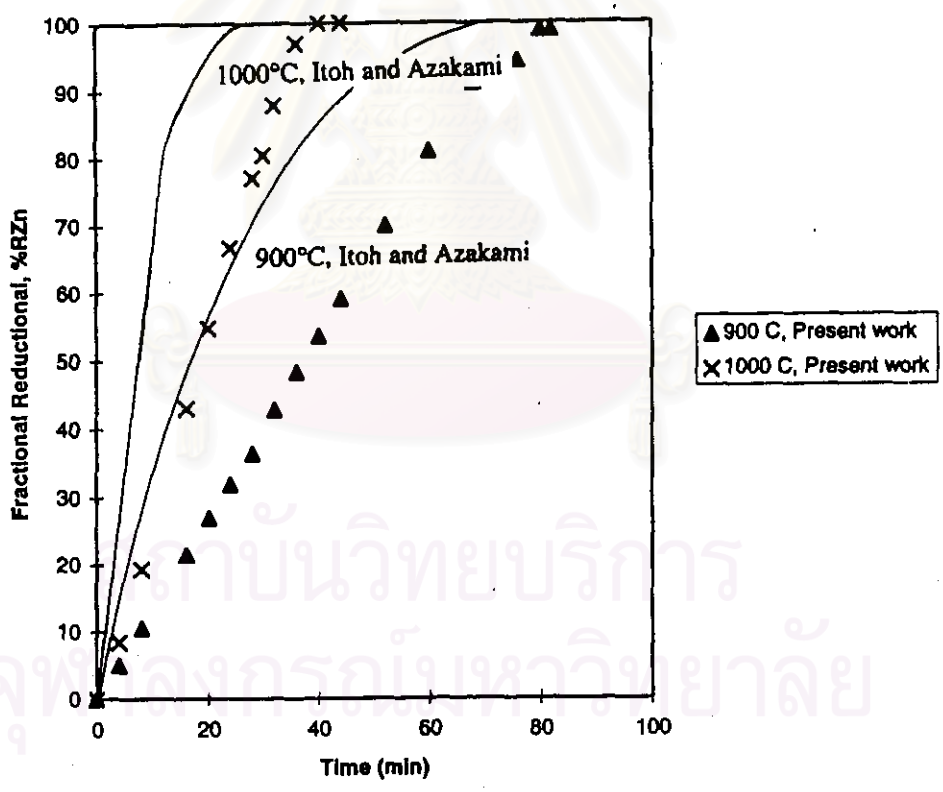

Figure 7.2: Comparison of the second reduction stage results.

In this reduction stage, the lead, sodium, potassium and chlorine percentage decreased after reduction. The cadmium percentage was the same as obtained after the first reduction stage. The reduced briquettes were examined by the ICP-AES method and the results are shown in Table 6.5 (see page 71).

All of these results were obtained by weight loss measurement and assumed that zinc is the only volatile element. Table 6.5 shows that not only zinc but also lead, sodium, potassium and chlorine were also volatile. The residue obtained from reduction in a nitrogen atmosphere at 1200 °C for 4 hours still contained 0.38 percent of zinc but according to the results in Figure 6.7 zinc oxide was completely reduced. Therefore, the results obtained by the weight loss measurement may be in error by about 2.0 percent.

Apparently, the lead percentage after reduction under vacuum was lower than in a nitrogen atmosphere. Since lead has a relatively high boiling point (T_{bp}=1620 °C) compared to the other volatile constituents of the EAF dust, the reduced lead will be present as a liquid at partial pressures of lead above its equilibrium vapour pressure. That is, the lead is reduced to a vapour phase only at partial pressures of lead below $1.8*10^{-3}$ atm at 1000 °C and $1.8*10^{-2}$ atm at 1200 °C.

From Table 6.5, it was found that the percentage of lead, sodium, potassium and chlorine also decreased. Sodium and potassium form chlorides which evaporate separately from zinc vapour. Therefore the zinc vapour product would be contaminated with lead. If the zinc oxide in the unreacted dust was 100 percent reduced, the zinc vapour product would have 5.5 to 7.6 percent of lead (see the calculation from Appendix G) contaminated after reduction. Further processing would be needed to separate lead from the zinc product. On the other hand, dust could be washed by water to leach the halides before reduction and the zinc-lead volatiles could be condensed using a lead-splash condenser.

7.4.2 Formulation of a Kinetic Model

The experimental data were analysed by applying some kinetic models in order to clarify the kinetic behavior of reduction in a nitrogen atmosphere and under vacuum.

The grain model for a solid undergoing reaction (Szekely *et al.*, 1976) was used to explain the mechanism of zinc oxide reduction with metallic iron. The reaction occurs throughout the whole briquette. The reaction steps are proposed as follows :

1) The chemical reaction step at the zinc oxide and metallic iron particle interface.
2) The zinc vapour diffuses through the pores between the particles to the briquette surface and transfers from the surface to the nitrogen atmosphere or vacuum.

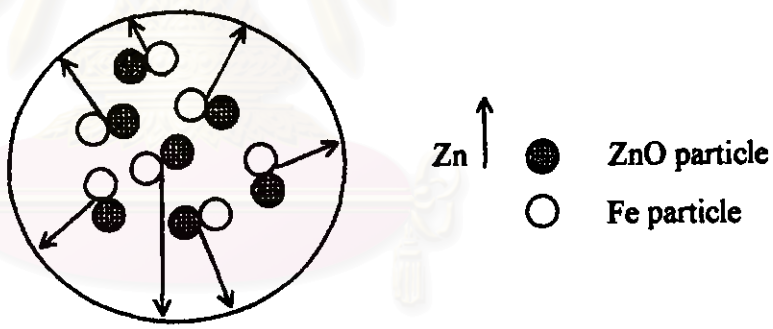

Figure 7.3: The grain model for zinc oxide reduction with metallic iron.

a) In Nitrogen Atmosphere

Equations for three different kinetic models were applied to the results obtained from Figure 6.7 . As shown in Figures 7.4 and 7.5, the relationship between time and $1-(1-F)^{1/3}$ and $1-2F/3-(1-F)^{2/3}$, where F is the fractional reduction, are almost linear for the results at the temperatures from 900 to 1200 °C. Figure 7.4 shows that the relationship between time and $1-(1-F)^{1/3}$ gives a better fit over the range 900 to 1200°C.

The slope of the linear portion of the reduction and time curve is equivalent to the rate constant, k. The rate constant was also calculated in units of percent reduction per second.

According to Arrhenius' law, a plot of the natural logarithm of k (ln k) versus the inverse of the reaction temperature, 1/T, gives a straight line, and the activation energy (E_A) of the reaction can be calculated from the slope of the line which is equal to $-E_A/R$, where R is the gas constant (8.314 J/mol K). The plot of ln k versus 1000/T is presented in Figure 7.6 for the k values obtained from Figure 7.4 . The activation energy of the reaction was found to be 141.65±8.20 kJ/mol. This quite high activation energy value indicates that the reaction rate may be limited by chemical or mixed control mechanisms.

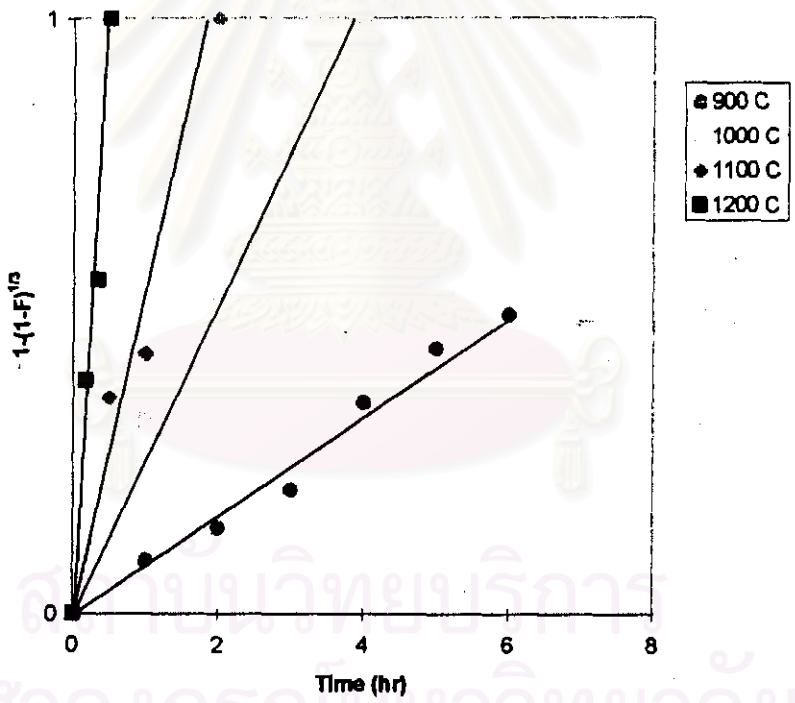

Figure 7.4: Plot of experimental data in nitrogen atmosphere by the chemical control mechanism.

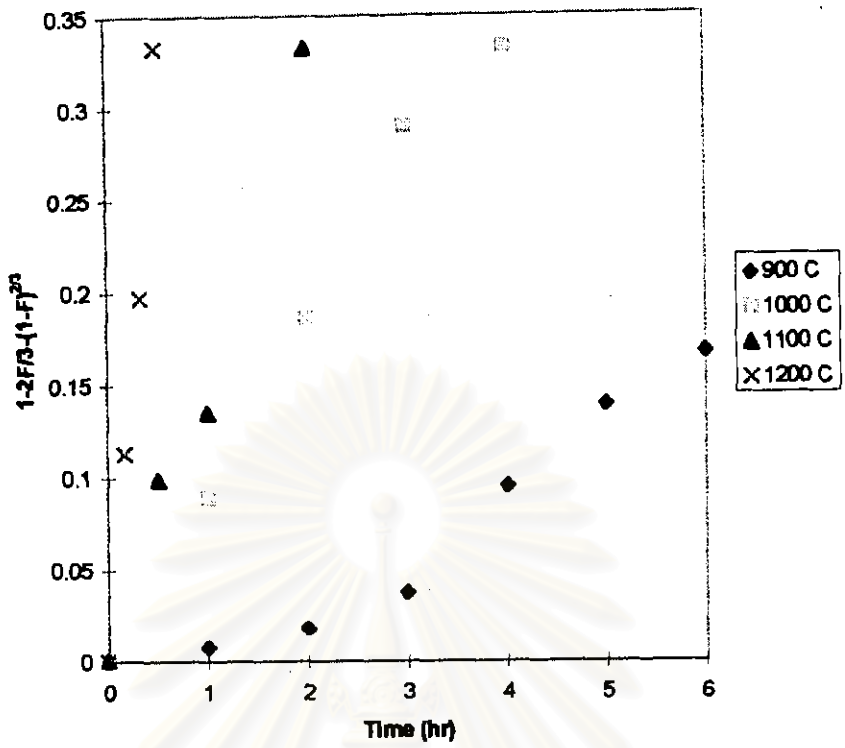

Figure 7.5: Plot of experimental data in nitrogen atmosphere by the diffusion control mechanism.

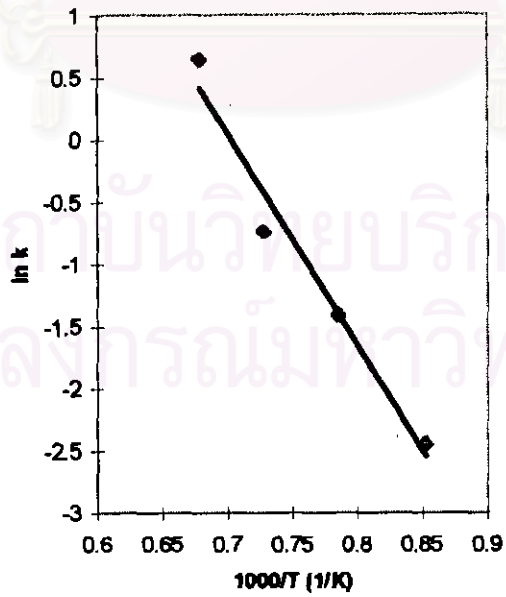

Figure 7.6: Arrhenius plot of ln k *vs* 1000/T (in nitrogen atmosphere) obtained from the chemical control mechanism.

Figure 7.7 shows the parabolic rate law applied to the results obtained from Figure 6.7. It was found that the relationship between time and F^2 does not give a straight line.

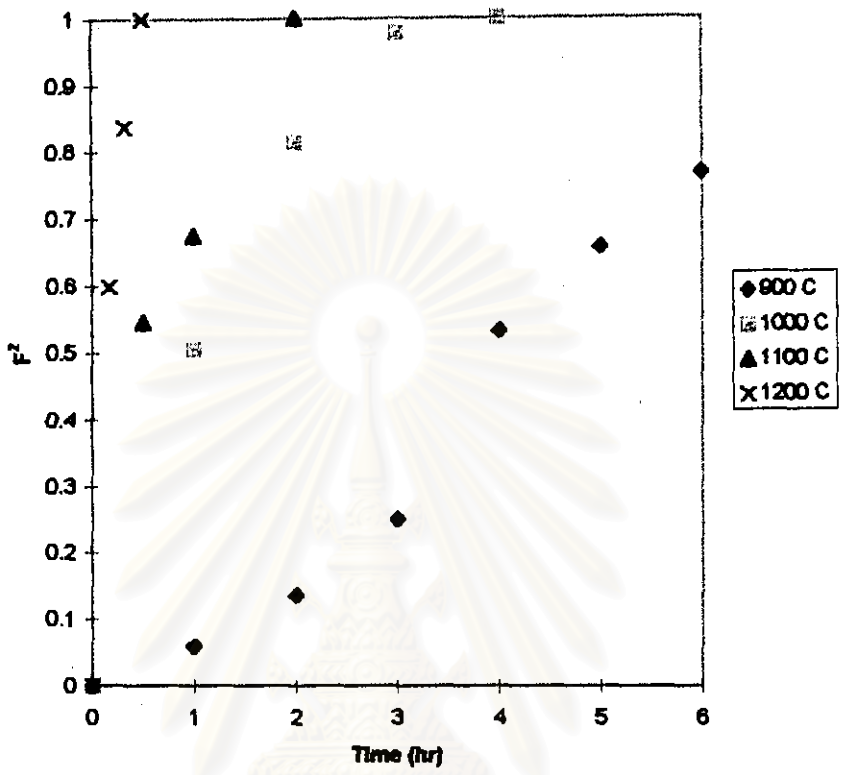

Figure 7.7: Plot of experiment data in nitrogen atmosphere by the parabolic rate law.

b) Under Vacuum

Figure 6.8 (see page 69) shows that the reduction rates were linear with time up to 80 percent reduction. The activation energy of the reduction rates under vacuum was calculated by using the initial slope of the linear portion of the reduction versus time curve which is equivalent to the initial rate constant, k (obtained from the results Figure 6.8). The rate constant was calculated in units of percent reduction per second. A plot of the natural logarithm of the rate constant (ln k) *vs* 1000/T of the reduction under vacuum is shown in Figure 7.8. The activation energy was found to be 69.83±8.20 kJ/mol. This relatively low activation energy may indicate a diffusion-controlled process.

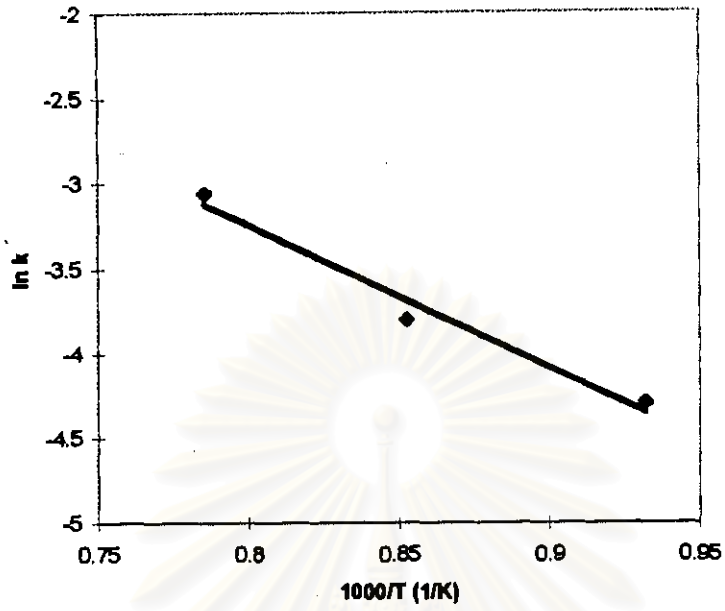

Figure 7.8: Arrhenius plot of ln k *vs* 1000/T (under vacuum).

c) Comparison of reduction rates in a nitrogen atmosphere and under vacuum

Figure 6.9 (see page 70) shows that the reduction rates under vacuum are significantly faster than in a nitrogen atmosphere for both temperatures. Figure 6.10 (see page 72) shows that zinc concentration decreases from the centre to the edge of the briquette for both samples (in nitrogen and vacuum). Under vacuum the zinc level decreases more than in a nitrogen atmosphere. Both of these results support the following reaction mechanism. The zinc oxide reacts with metallic iron at the particle interface throughout the briquette. Zinc vapour then diffuses through the pores and is transferred from the briquette surface to nitrogen or vacuum.

The increased rate of transfer of zinc vapour under vacuum promotes a faster reduction rate.